JACS
JOURNAL OF THE AMERICAN CHEMICAL SOCIETY

ARTICLE

pubs.acs.org/JACS

Bivalent Inhibitors for Disrupting Protein Surface-Substrate Interactions and for Dual Inhibition of Protein Prenyltransferases

Shinnosuke Machida,[†] Nobuo Kato,[†] Kazuo Harada,[‡] and Junko Ohkanda*[,†]

[†]The Institute of Scientific and Industrial Research, Osaka University, 8-1 Mihogaoka, Ibaraki, Osaka 567-0047, Japan

[‡]Department of Life Sciences, Tokyo Gakugei University, Koganei, Tokyo 184-8501, Japan

Supporting Information

ABSTRACT: Low-molecular-weight compounds that disrupt protein−protein interactions (PPIs) have tremendous potential applications as clinical agents and as chemical probes for investigating intracellular PPI networks. However, disrupting PPIs is extremely difficult due to the large, flat interfaces of many proteins, which often lack structurally defined cavities to which drug-like molecules could bind in a thermodynamically favorable manner. Here, we describe a series of bivalent compounds that anchor to the enzyme active site to deliver a minimally sized surface-binding module to the targeted surface involved in transient PPI with a substrate. These compounds are capable of significantly inhibiting enzymatic reactions involving protein surface−substrate interaction in the single-digit nanomole range. Inhibitors of farnesyltransferase (FTase), which possesses a negatively charged local area on its α-subunit, were designed by attaching a module derived from a branched monoamine-containing gallate to a conventional active-site-directed CVIM tetrapeptide using an alkyl spacer. A significant improvement in inhibitory activity (>200-fold) against farnesylation of the K-Ras4B peptide was observed when the gallate module was attached to the CVIM tetrapeptide. Furthermore, the bivalent compounds had submicromolar inhibitory activity against geranylgeranylation of the K-Ras4B peptide catalyzed by GGTase I, which has an α-subunit identical to that of FTase. The anchoring strategy we describe would be useful for designing a new class of PPI inhibitors as well as dual enzyme inhibitors targeting common surface structures.

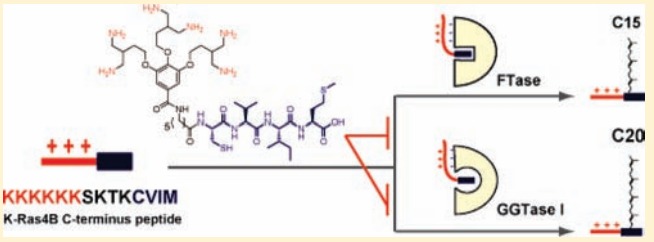

INTRODUCTION

Protein−protein interactions (PPIs) mediate the signaling networks that regulate numerous biological processes. Disruption of PPIs by synthetic agents has been a major goal of recent pharmacological research efforts due to the rich potential for the development of new therapeutic agents for many diseases, including cancer and central nervous system diseases.[1−3] However, progress in this field has not come easily, because PPIs often involve large and flat interfaces that lack precise structural features. Examples of successful PPI disrupting agents include some synthetic compounds,[4,5] cyclic peptide and peptidomimetic-based agents,[6,7] β-peptides,[8,9] and quadruplexes and aptamers.[10,11] These agents almost exclusively employ a rigid scaffold that generates large antibody-like agents. However, delivering drug-like small molecules targeted to the large surface area of proteins remains a difficult challenge.

Using a simple anchoring strategy, it may be possible to deliver minimally sized small agents to targeted area on the surface of proteins in order to disrupt PPIs. Bivalent compounds would be particularly beneficial in disrupting PPIs involving enzymes and their substrate proteins, as they can exploit the enzyme active sites for both anchoring and selective binding. Here, we report the first bivalent inhibitors that disrupt a transient PPI model of protein prenyltransferases. Furthermore, we provide evidence that these compounds exhibit dual inhibition activity for farnesyltransferase (FTase) and its functionally related enzyme, type-I geranylgeranyltransferase (GGTase I), by recognizing their common acidic surface.

Transient PPIs with a short half-life (0.1−1 s) play a crucial role in substrate recognition by enzymes implicated in many posttranslational modifications.[12−14] Although the mechanisms of most transient PPIs remain unknown because of their relatively low affinity (K_d = 10^{-6}−10^{-5} M), recent biological studies have revealed that the transient PPIs involving the MAPK family[12] and phosphatase Cdc25B[13,14] are driven by electrostatic interactions. Therefore, we hypothesized that blocking the surface to prevent substrate binding and/or neutralizing the surface charge using a synthetic agent consisting of complementary functional groups might disrupt such transient PPIs.

Protein prenylation is a lipid posttranslational modification of many proteins, and disrupting this modification has become a major clinical focus for many diseases over the past few decades.[15−17] Two protein prenyltransferases have received considerable attention for their potential in treating cancers. The structurally related FTase and GGTase I attach a C15 farnesyl or a C20 geranylgeranyl group to a thiol group on the C-terminal CAAX tetrapeptide (C = cysteine, AA = aliphatic dipeptide, X = Met, Ser, Gln for FTase,

Received: September 23, 2010
Published: December 15, 2010

Leu, Phe for GGTase I) of corresponding substrate proteins.[18] A recent genetic study showed that simultaneous inactivation of FTase and GGTase I markedly reduces the size of lung tumors in mice, suggesting that dual inhibitors of both enzymes would be valuable cancer therapeutic agents.[17] FTase and GGTase I are heterodimeric zinc metalloenzymes consisting of identical 48 kDa α-subunits that are products of the same gene (Figure 1). Importantly, on the α-subunit surface near the entrance of each active pocket, there is an approximately 90 Å^2 negatively charged area where a number of acidic amino acids (Glu125, Glu160, Glu161, Glu187, Asp191, Glu229, and Asp230) are clustered.[19]

Human K-Ras4B is the most frequently mutated Ras isoform in cancers. This protein is normally farnesylated by FTase at the thiol group of the C-terminal CVIM sequence (Figure 2a). However, disruption of K-Ras4B farnesylation by FTase inhibitors causes an alternative geranylgeranylation by GGTase I (Figure 2b), which enables K-Ras4B to retain full biological activity.[20,21] Biological studies[22−25] and studies based on crystal structures[19] have demonstrated that a critical determinant for the unusual geranylgeranylation of K-Ras4B is the characteristic polylysine sequence near the protein's carboxyl terminus. This highly positively charged region has been thought to trigger a transient PPI with the acidic surfaces of FTase and GGTase I through an electrostatic interaction (Figure 2).[19−25] The PPI was confirmed by K-Ras4B's unusually higher affinity (20−50 times) for FTase than that of H-Ras isoform.[22,23] On the basis of these results, we predicted that a compound mimicking the C-terminal structure of K-Ras4B would simultaneously bind to the active site and the acidic surface of both FTase and GGTase I and block the transient PPI, resulting in inhibition of both farnesylation and geranylgeranylation of K-Ras4B.

In this paper, we describe the rational design of K-Ras4B mimetics for prenyltransferase inhibitors and evaluate their function in PPI disruption. We also discuss the dual inhibition of FTase and GGTase I, as well as the structural requirements for mimetic binding to the protein surface.

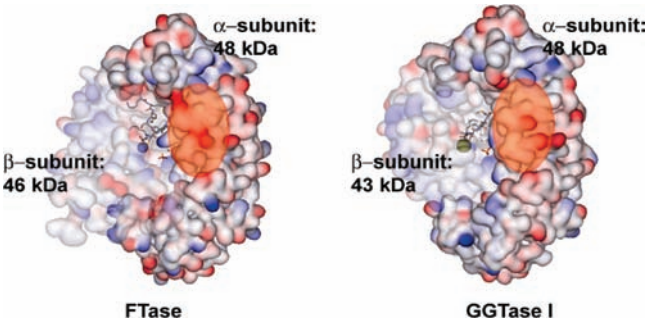

Figure 1. Crystal structures of the ternary complex of mammalian FTase (1D8D) and GGTase I (1N4Q) bound to peptide substrate and prenyldiphosphate analogues. Negatively charged and positively charged surfaces are shown in red and blue, respectively. The acidic areas of α-subunits are highlighted with a red circle.

RESULTS AND DISCUSSION

Design of Bivalent FTase Inhibitors. In order to design bivalent inhibitors based on the C-terminal structural features of K-Ras4B, we applied a module assembly approach, in which small module compounds are designed to recognize a specific local protein surface area and are assembled by covalent linking[26] or metal chelation.[27] As shown in Scheme 1, the characteristic 14-amino-acid sequence of the K-Ras4B C-terminus (KKKKKKSKTKCVIM) was divided into three sections: the lysine hexamer (K_6), a tetrapeptide linkage, and the CAAX motif, CVIM. The lysine hexamer, tetrapeptide linkage, and CAAX motif were replaced by a module compound designed for surface binding, a spacer, and an anchor, respectively. For the anchoring module, we initially chose the CVIM tetrapeptide to ensure that the module would bind to the FTase active site. To mimic the $(K)_6$ section, we used a gallate scaffold,[26] and the same number of primary amino groups were introduced using branched alkyl amines. A computer-generated superimposed model suggested that the gallate module was nearly comparable in size to the local acidic area of the FTase surface and that ~12 Å would be an appropriate length for the spacer (Supporting Information, Figure S1). The modules were thus linked by either a C5 alkyl spacer or an ethylene glycol chain, $(CH_2CH_2O)_2CH_2$, to produce compounds **1a** and **1b**, as shown in Scheme 1. For comparison, we also synthesized various bivalent compounds in which the number of amino groups was reduced by half (Scheme 1, compound **2**), the amino groups were replaced by carboxyl groups (Scheme 1, compound **3**), or the CVIM anchor was replaced by a more

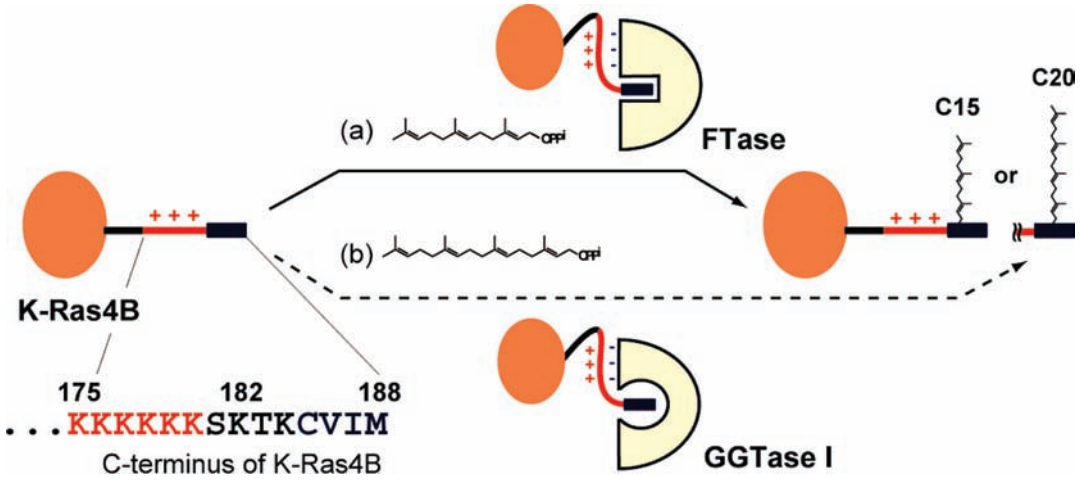

Figure 2. Schematic representation of K-Ras4B prenylation. Interaction between K-Ras4B and FTase/GGTase I involves electrostatic surface interactions.

dx.doi.org/10.1021/ja1086112 |J. Am. Chem. Soc. 2011, 133, 958–963

Scheme 1. The 14-Amino-Acid Sequence of the K-Ras4B C-Terminus, Divided into Three Sections for the Module Design, and the Structures of Compounds Tested in This Study[a]

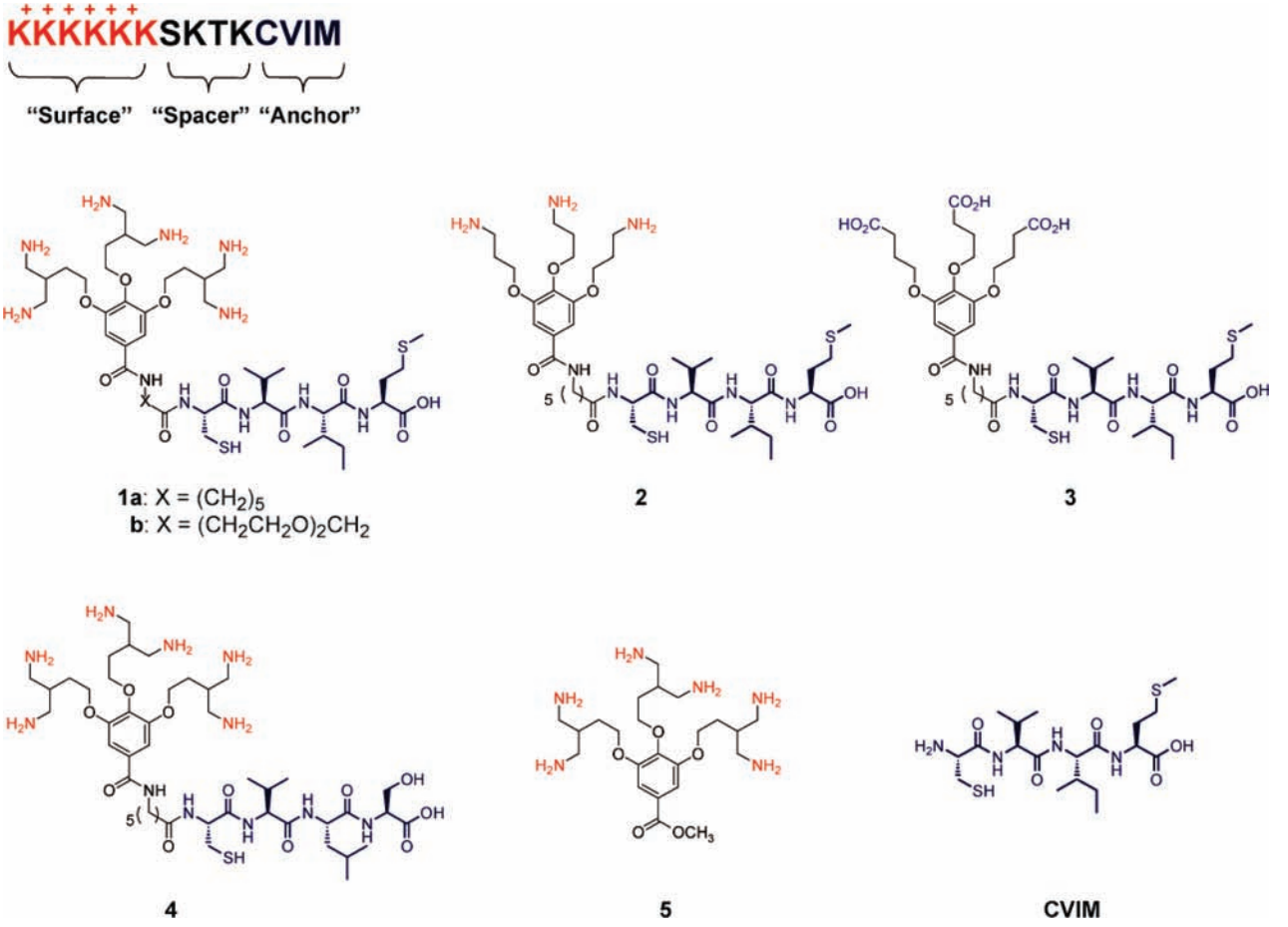

[a] The lysine hexamer (red), a tetrapeptide linkage (black), and the CVIM (blue) were replaced by a gallate module containing amino groups (red) or carboxylates (blue), an alkyl or ethylene glycol spacer (black), and the tetrapeptide CVIM or CVIS (blue), to give the bivalent compounds **1**−**4**, respectively. Gallate **5** and CVIM were also prepared as controls.

hydrophilic tetrapeptide (CVLS), which is the H-Ras CAAX motif (Scheme 1, compound **4**). Gallate methyl ester (Scheme 1, compound **5**) and the tetrapeptide CVIM were also prepared as controls.

Prenylation of Dansylated K-Ras4B Peptide. To evaluate the disruption of the PPI between K-Ras4B and FTase, the mimetic compounds were tested using a fluorescent enzyme assay[28] modified to incorporate an environmentally sensitive fluorogenic substrate, a dansylated oligopeptide truncated from the K-Ras4B C-terminal sequence (KKKKKKSK(Dans)-TKCVIM). The K182 ω-amino group was chosen for the dansyl modification, as analysis of the previously reported crystal structure of the ternary complex of FTase bound to KKKSKTKCVIM and an analogue of farnesyl pyrophosphate (FPP)[19] suggested that this position would not interfere with CVIM binding to the active site. Our first objective was to carefully assess whether the dansylated K-Ras4B peptide could be used as a model for K-Ras4B farnesylation. Previous studies[22,23] reported that K-Ras4B possesses a notably higher affinity for FTase than other Ras isoforms, such as H-Ras, due to the presence of a polylysine region (K_m for K-Ras4B = 0.03 μM, K_m for H-Ras = 0.6 μM). A Michaelis−Menten analysis of farnesylation of the K-Ras4B peptide gave a K_m value of 0.006 ± 0.002 μM (Figure 3A), which was 2 orders of magnitude lower than that for the *N*-dansylated pentapeptide lacking the polylysine domain (DansGCVIM, K_m = 0.539 ± 0.057 μM). This apparent shift in the K_m values for FTase demonstrates that the interaction is promoted by the basic domain of the K-Ras4B peptide and the acidic surface of FTase. Furthermore, as shown in Figure 3B, the K-Ras4B peptide was also a GGTase I substrate with decent affinity, whereas geranylgeranylation of DansGCVIM proceeded less efficiently (K_m = 0.033 ± 0.008 μM for the K-Ras4B peptide and 0.956 ± 0.374 μM for DansGCVIM). These results validate the use of dansylated K-Ras4B peptide as a model for K-Ras4B prenylation involving transient PPI with FTase and GGTase I.

Inhibition of Farnesylation of the K-Ras4B Peptide. Next, we evaluated the inhibitory activity of the bivalent compounds against farnesylation of the K-Ras4B peptide. The resulting IC_{50} values were converted to inhibition constants (K_i) using the Cheng−Prusoff equation.[29] The results are shown in Figure 4 and summarized in Table 1. The tetrapeptide CVIM inhibited FTase only moderately, as evidenced by its micromolar K_i value. Compound **1a**, on the other hand, demonstrated an extremely high potency, with a K_i value in the low nanomolar range (IC_{50} = 0.85 μM and K_i = 0.005 ± 0.001 μM), and was more than 200 times more effective at inhibiting farnesylation than CVIM

dx.doi.org/10.1021/ja1086112 |*J. Am. Chem. Soc.* 2011, 133, 958–963

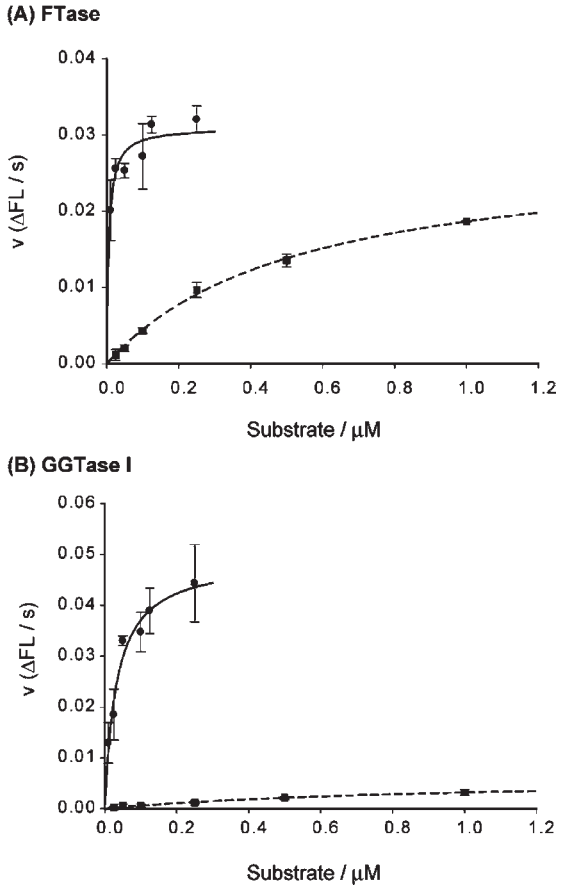

Figure 3. Michaelis–Menten analysis of the affinity of the K-Ras4B peptide KKKKKKSK(Dans)TKCVIM (●, —) and DansGCVIM (■, ---) for (A) FTase and (B) GGTase I. Standard deviation values are given for $n = 3$.

(IC_{50} = 182 μM and K_i = 1.10 ± 0.29 μM). A Lineweaver–Burk analysis shows that the inhibition mode of compound **1a** is competitive (Figure S2), and the K_i value obtained from the plot (K_i = 0.002 μM) was consistent with the data derived from the Cheng–Prusoff equation as described above.

Bivalent compound **2**, which contains fewer amino groups than compound **1a**, was approximately 5-fold less active than **1a**, demonstrating that the number of amino groups affects the inhibitory potency (compound **2** IC_{50} = 4.8 μM). Gallate-derivative compound **5** showed no inhibitory activity (0% inhibition at 100 μM; see also Figure S3). These results suggest that the cationic gallate module of compound **1a** interacts with the acidic surface of FTase, resulting in greater potency in inhibiting farnesylation of the K-Ras4B peptide compared to CVIM alone. Two plausible explanations for the enhanced potency of the gallate module are that the polycationic moiety (1) blocks the acidic surface and prevents substrate binding or (2) neutralizes the net charge of the acidic surface, resulting in a decrease in the Coulomb attraction between FTase and the cationic model peptide. The latter explanation may be the most plausible, because in general protein binding involving electrostatic interactions plays a role in the rate of docking but is less important in contributing to the binding energy.[30]

Dual Inhibition of Prenylation of the K-Ras4B Peptide. Since the bivalent compounds were proven to be potent inhibitors of FTase, we then examined whether the compounds

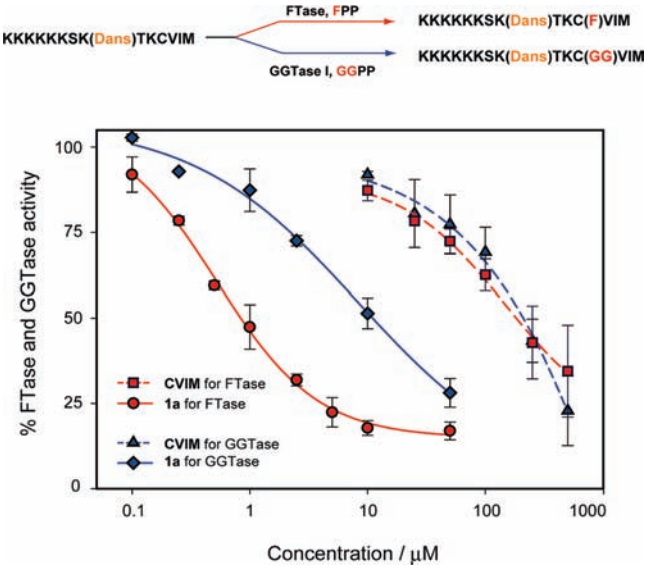

Figure 4. Dose–response curves for the inhibition of FTase (red) by the peptide CVIM (squares) and compound **1a** (circles), and inhibition of GGTase-I (blue) by the peptide CVIM (triangles) and **1a** (diamonds). Fluorescent in vitro assays were carried out by using KKKKKKSK-(Dans)TKCVIM (1 μM) and FPP (5 μM) in 50 mM Tris-HCl, pH 7.5, at 30 °C. The standard deviation values are given for $n = 3$.

Table 1. Inhibition of Prenylation of the K-Ras4B Model Peptide

	K_i, μM[a]	
compd	FTase	GGTase I
1a	0.005 ± 0.001	0.344 ± 0.086
2	0.028 ± 0.008	0.479 ± 0.119
4	0.008 ± 0.001	>1.6
5	>100	n/a
CVIM	1.10 ± 0.29	6.69 ± 1.67

[a] K_i values were obtained by conversion of IC_{50} values using the Cheng–Prusoff equation: $K_i = IC_{50}/\{1 + ([S]/K_m)\}$. Standard deviation values are given for $n = 3$.

possessed any dual inhibitory activity against GGTase I, which also possesses an acidic area near the active site (Figure 1). To answer this question, we monitored geranylgeranylation of the K-Ras4B peptide under various concentrations of each compound. As shown in Figure 4, compound **1a** indeed inhibited the geranylgeranylation with submicromolar potency, while CVIM showed only weak activity (Table 1; IC_{50} = 10.8 μM and K_i = 0.344 ± 0.086 μM for compound **1a**; IC_{50} = 210 μM and K_i = 6.69 ± 1.67 μM for CVIM). These results suggest that attaching the gallate module converts the ineffective CVIM peptide into a reasonably effective GGTase I inhibitor. Interestingly, the improved potency brought about by introducing the gallate module was significant in the case of FTase (220 times greater potency), whereas introduction of the gallate module had only a moderate on inhibition of GGTase I (~20 times greater potency). A possible explanation for this observation is that the spacer length might provide for a better fit between the gallate module and FTase than it does for GGTase I. It is noteworthy that CVLS-containing bivalent compound **4** was equally active as compound

dx.doi.org/10.1021/ja1086112 |J. Am. Chem. Soc. 2011, 133, 958–963

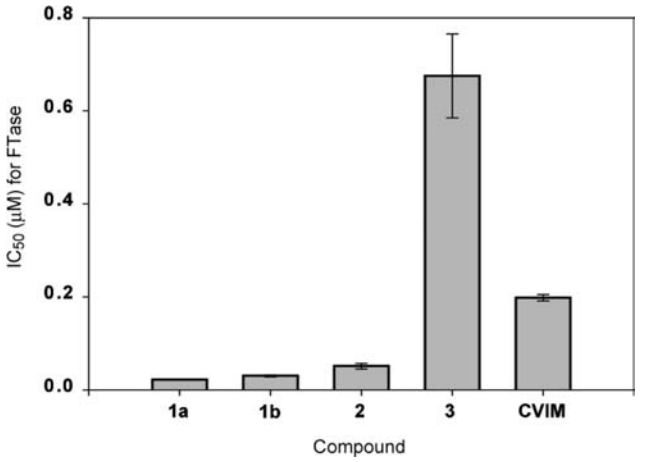

Figure 5. IC_{50} values (μM) of compounds tested for FTase inhibition activity. Fluorescent in vitro assays were carried out by using DansGCVIS (1 μM) and FPP (5 μM) in 50 mM Tris-HCl, pH 7.5, at 30 °C. The standard deviation is given for $n = 3$.

1a in inhibiting FTase; however, compound **4** did not significantly inhibit GGTase I (Table 1). This observation is consistent with a previous study[22] demonstrating that GGTase I attaches a geranylgeranyl group to K-Ras4B, but not to H-Ras, presumably because the hydrophilic serine residue decreases the binding affinity for the active site of GGTase I, which is more hydrophobic than that of FTase.[31] Although a number of studies have reported dual inhibition of FTase/GGTase I,[17,32−34] to the best of our knowledge, ours is the first report describing rationally designed dual inhibitors of FTase and GGTase I that target the same acidic surface structure.

Gallate Module Functional Groups Affect Inhibitory Potency against FTase. To systematically evaluate the effect of functional groups introduced into the gallate scaffold on FTase inhibition, we compared IC_{50} values between various bivalent compounds and modules. Compounds were screened by a conventional method[28] using a short peptide, *N*-dansylated GCVIS (DansGCVIS). The resulting IC_{50} values are summarized in Figure 5 (also see Figure S4). Compared to CVIM, which inhibited FTase with an IC_{50} value of 0.198 ± 0.007 μM, the IC_{50} values for compounds **1a** and **1b** were approximately 1 order of magnitude lower (**1a**, $IC_{50} = 0.022 \pm 0.001$ μM; **1b**, $IC_{50} = 0.030 \pm 0.002$ μM), indicating that these compounds were considerably more potent at inhibiting FTase, and confirming the synergetic effect of the gallate introduced in **1a** and **1b** upon binding to the enzyme. Changes in the length of the spacer had little effect on the activity, as both compounds **1a** and **1b** had similar activities. Gallate methyl ester compound **5** was again found to be inactive (0% inhibition at 100 μM; see Figure S3). Thus, the relatively small gallate module incorporated in compound **1** is a very weak binder by itself and contributes to an increase in inhibitory activity only by being anchored and delivered to the flat acidic surface. As seen with compound **2**, a decrease in the number of amino groups in the gallate module slightly diminished the inhibitory activity ($IC_{50} = 0.051 \pm 0.006$ μM). More convincing evidence for the binding of gallate to the protein surface was obtained when the amino groups in compound **2** were replaced with carboxylic acids to afford compound **3**. Compound **3** had a significantly diminished inhibitory activity against FTase, with an IC_{50} (0.675 ± 0.090 μM) that was more than 1 order of magnitude higher than that of compound **2**, and compound **3** was approximately 3.5 times weaker than CVIM (Figure 5). These results provide strong evidence of electrostatic repulsion between the module and the protein surface.

CONCLUSIONS

By mimicking the K-Ras4B C-terminal structure, we designed and synthesized the first bivalent dual inhibitors of FTase and GGTase I. We covalently linked two modules that recognize the active sites and the identical acidic surfaces of the α-subunits of FTase and GGTase I. Compound **1a** displayed remarkable inhibitory potency, with a K_i of 5 nM for farnesylation of the K-Ras4B peptide, and was 220 times more effective than the tetrapeptide module, CVIM. Furthermore, compound **1a** suppressed geranylgeranylation of the K-Ras4B peptide at submicromolar concentrations. On the basis of these results, we conclude that the cationic surface-binding module, which displays no inhibitory activity by itself, is delivered to the targeted protein surface by anchoring and efficiently disrupts the interaction between the K-Ras4B peptide and the FTase surface. The strategy described in this paper may provide a general method for designing inhibitors of transient PPIs, especially in the case of enzymes for which the anchoring positions, such as deep clefts, are accessible (i.e., the active pocket). Our results also suggest that identical and/or similar surface characteristics between isozymes or members of enzyme families make such proteins vulnerable to dual inhibitors.

The bivalent compounds described in this paper were designed to specifically inhibit K-Ras4B prenylation. We do not expect that these CVIM anchor compounds would interfere with normal geranylgeranylation processing, because GGTase I native substrate proteins possess CAAX motifs that are more favorably recognized by GGTase I than CVIM. If such selective K-Ras4B inactivation becomes possible, strategies based on K-Ras4B mimicry of the protein surface may lead to less toxic dual inhibitors, which would be clinically important since the dual inhibitors of FTase and GGTase I reported thus far cause severe toxicity in animals.[32]

Toward this goal, peptidomimetic modifications of the CVIM module and functional evaluation of these compounds in cells are currently underway in our laboratory.

MATERIALS AND METHODS

Materials and Instruments. Reagents and solvents were obtained from commercial sources without further purification, unless otherwise noted. ^{1}H and ^{13}C NMR spectra were recorded on a JEOL JNM-LA 400 spectrometer. Chemical shifts were reported in δ (ppm) relative to tetramethylsilane. All coupling constants were described in Hz. Elemental analyses were performed by Mr. T. Matsuzaki using a Perkin-Elmer 2400CHN instrument in the Material Analysis Center of ISIR. Flash column chromatography was performed on silica gel (40−63 μm) under a pressure of about 4 psi. HPLC analysis was performed using a JASCO PU-2086 liquid chromatograph and a JASCO UV-2075 detector with a GL Science Inertsil 150 mm × 4.6 mm, 5 μm C-18 column, eluted with a gradient from 10% to 90% acetonitrile in 0.1% trifluoroacetic acid over 30 min. High-resolution mass spectra (HRMS) and low-resolution mass spectra (LRMS) were acquired at the Nagasaki University Instrument Center. The K-Ras4B model peptide (KKKKKKSK(Dans)TKCVIM) was purchased from the Toray Research Center. The enzyme inhibition assays were performed using a Shimadzu RF-5300PC spectrofluorophotometer with a temperature controller (Sansyo SA-100).

The procedures for synthesizing compounds **1**−**5** and CVIM, along with a detailed characterization of each, are described in the Supporting Information.

Fluorescent Enzyme Inhibition Assay. Recombinant mammalian FTase and GGTase-I were expressed and purified using previously reported methods.[35] The inhibitory activity of the synthetic compounds against FTase and GGTase-I was measured using a previously described fluorescent assay[26] employing the fluorogenic substrates, DansGCVIS or KKKKKKSK(Dans)TKCVIM, respectively. A peptide buffer (53 mM Tris-HCl, pH 7.5, 0.1 mM EDTA, 0.020% *n*-dodecyl β-maltoside, 5.0 mM DTT) was used for preparation of the fluorogenic substrate stock solution. An assay buffer (50 mM Tris-HCl, pH 7.5, 1.2 mM $MgCl_2$, 12 μM $ZnCl_2$, 0.023% *n*-dodecey β-D-maltoside, and 5 mM DTT) was used for enzyme dilution and for running the kinetic assay. FPP and GGPP ammonium salt methanol was purchased from Sigma-Aldrich and diluted to 500 μM with 25 mM NH_4HCO_3, stored at −80 °C in aliquots, and then further diluted to 110 μM before use (methanol content <3.3%). The peptide substrate, DansylGCVIS, was dissolved in peptide buffer (approximately 500 μM), the concentration determined from a standard curve of A_{340} versus the concentration of dansylglycine dissolved in peptide buffer. Inhibitors were initially dissolved in DMSO (5.0 mM except for CVIM, which was prepared at 2.0 mM), further diluted with peptide buffer to 500 μM, and stored at −80 °C in aliquots until used. These solutions were diluted to various concentrations (0.22−22 μM) for use in assays of inhibitory activity. The FTase stock solution (35.5 μM) was diluted with assay buffer immediately prior to use (1.78 μM). Assays were performed at 30 °C using a thermostatic cuvette holder. Ten microliter aliquots of FTase, FPP, and inhibitor were added to 180 μL of assay buffer solution in a 500-μL tube, which was then incubated in a 30 °C water bath for 5 min. The DansGCVIS solution (10 μL) was then added, the mixture was vortexed and quickly transferred to the cuvette, and the fluorescent intensity change at 520 nm (ex: 340 nm) was monitored for 5 min. The final concentrations of each component were as follow: DansGCVIS, 1 μM; FPP, 5 μM; FTase, 81 nM; inhibitor, 0−1000 nM (the content of DMSO in the final solution was less than 0.05%). The experiments for each concentration of inhibitor were repeated at least three times.

■ ASSOCIATED CONTENT

Supporting Information. Experimental details regarding compound synthesis, fluorescent kinetic assays (Figures S2−S4), and complete refs 6, 32, and 34. This material is available free of charge via the Internet at http://pubs.acs.org.

■ AUTHOR INFORMATION

Corresponding Author
johkanda@sanken.osaka-u.ac.jp

■ ACKNOWLEDGMENT

This work was supported by The Takeda Science Foundation, The Naito Memorial Foundation, and Eisai Corp. (J.O.). We thank Prof. A. D. Hamilton, Prof. S. M. Sebti, and Michelle A. Blaskovich for their helpful suggestions. Financial support to S. M. was provided by the GCOE program of Osaka University. DansGCVIM was prepared by C. Oura.

■ REFERENCES

(1) Wells, J. A.; McClendon, C. L. *Nature* **2007,** *450,* 1001–1009.
(2) Robinson, J. A.; DeMarco, S.; Gombert, F.; Moehle, K.; Obrecht, D. *Drug Discovery Today* **2008,** *13,* 944–951.
(3) Blazer, L. L.; Neubig, R. R. *Neuropsychopharmacology* **2009,** *34,* 126–141.
(4) Saraogi, I.; Hebda, J. A.; Becerril, J.; Estroff, L. A.; Miranker, A. D.; Hamilton, A. D. *Angew. Chem., Int. Ed.* **2010,** *49,* 736–739.
(5) Bach, A.; Chi, C. N.; Pang, G. F.; Olsen, L.; Kristensen, A. S.; Jemth, P.; Strømgaard, K. *Angew. Chem., Int. Ed.* **2009,** *48,* 9685–9689.
(6) Srinivas, N.; et al. *Science* **2010,** *327,* 1010–1013.
(7) Heinis, C.; Rutherford, T.; Freund, S.; Winter, G. *Nat. Chem. Biol.* **2009,** *5,* 501–507.
(8) Horne, W. S; Johnson, L. M.; Ketas, T. J.; Klasse, P. J.; Lu, M.; Moore, J. P.; Gellman, S. M. *Proc. Natl. Acad. Sci. U.S.A.* **2009,** *106,* 14751–14756.
(9) Michel, J.; Harker, E. A.; Tirado-Rives, J.; Jorgensen, W. L.; Schepartz, A. *J. Am. Chem. Soc.* **2009,** *131,* 6356–6357.
(10) Rosenzweig, B. A.; Ross, N. T.; Tagore, D. M.; Jayawickramarajah, J.; Saraogi, I.; Hamilton, A. D. *J. Am. Chem. Soc.* **2009,** *131,* 5020–5021.
(11) Kim, Y.; Cao, Z.; Tan, W. *Proc. Natl. Acad. Sci. U.S.A.* **2008,** *105,* 5664–5669.
(12) Tanoue, T.; Nishida, E. *Cell. Signal.* **2003,** *15,* 455–462.
(13) Rudolph, J. *Nature Rev. Cancer* **2007,** *7,* 202–211.
(14) Sohn, J.; Buhrman, G.; Rudolph, J. *Biochemistry* **2007,** *46,* 807–818.
(15) Kazi, A.; Carie, A.; Blaskovich, M. A.; Bucher, C.; Thai, V.; Moulder, S.; Peng, H.; Carrico, D.; Pusateri, E.; Pledger, W. J.; Berndt, N.; Hamilton, A. D.; Sebti, S. M. *Mol. Cell. Biol.* **2009,** *29,* 2254–2263.
(16) Gelb, M. H.; Brunsveld, L.; Hrycyna, C. A.; Michaelis, S.; Tamanoi, F.; Boorhis, W. C. V.; Waldmann, H. *Nat. Chem. Biol.* **2006,** *2,* 518–528.
(17) Liu, M.; Sjogren, A-K. M.; Karlsson, C.; Ibrahim, M. X.; Andersson, K. M. E.; Olofsson, F. J.; Wahlstrom, A. M.; Dalin, M.; Yu, H.; Chem, Z.; Yang, S. H.; Young, S. G.; Bergo, M. O. *Proc. Natl. Acad. Sci. U.S.A.* **2010,** *107,* 6471–6476.
(18) Casey, P. J.; Seabra, M. C. *J. Biol. Chem.* **1996,** *271,* 5289–5292.
(19) Long, S. B.; Casey, P. J.; Beese, L. S. *Structure* **2000,** *8,* 209–222.
(20) Whyte, D. B.; Kirschmeier, P.; Hockenberry, T. N.; Nunez-Oliva, I.; James, L.; Catino, J. J.; Bishop, W. R.; Pai, J. *J. Biol. Chem.* **1997,** *272,* 14459–14464.
(21) Rowell, C. A.; Kowalczyk, J. J.; Lewis, M. D.; Garcia, A. M. *J. Biol. Chem.* **1997,** *272,* 14093–14097.
(22) James, G. L.; Goldstein, J. L.; Brown, M. S. *J. Biol. Chem.* **1995,** *270,* 6221–6226.
(23) Zhang, F. L.; Kirschmeier, P.; Carr, D.; James, L.; Bond, R. W.; Wang, L.; Patton, R.; Windsor, W.; Syto, R.; Zhang, R.; Bishop, W. R. *J. Biol. Chem.* **1997,** *272,* 10232–10239.
(24) Smalera, I.; Williamson, J. M.; Baginsky, W.; Leiting, B.; Mazur, P. *Biochim. Biophys. Acta* **2000,** *1480,* 132–144.
(25) Fiordalisi, J. J.; Johnson, R. L., II; Weinbaum, C. A.; Sakabe, K.; Chen, Z.; Casey, P. J.; Cox, A. D. *J. Biol. Chem.* **2003,** *278,* 41718–41727.
(26) Machida, S.; Usuba, K.; Blaskovich, M. A.; Yano, A.; Harada, K.; Sebti, S. M.; Kato, N.; Ohkanda, J. *Chem.—Eur. J.* **2008,** *14,* 1392–1401.
(27) Ohkanda, J.; Satoh, R.; Kato, N. *Chem. Commun.* **2009,** 6949–6951.
(28) Pompiliano, D. L.; Gomez, R. P.; Anthony, J. J. *J. Am. Chem. Soc.* **1992,** *114,* 7945–7946.
(29) Cheng, Y.; Prusoff, W. H. *Biochem. Pharmacol.* **1973,** *22,* 3099–3108.
(30) Miyashita, O.; Onuchic, J. N.; Okamura, M. Y. *Biochemistry* **2003,** *42,* 11651–11660.
(31) Lane, K. T.; Beese, L. S. *J. Lipid Res.* **2006,** *47,* 681–699.
(32) Lobell, R. B.; et al. *Cancer Res.* **2001,** *61,* 8758–8768.
(33) deSolms, S. J.; Ciccarone, T. M.; MacTough, S. C.; Shaw, A. W.; Buser, C. A.; Ellis-Hutchings, M.; Fernandes, C.; Hamilton, K. A.; Huber, H. E.; Kohl, N. E.; Beese, L. S.; Taylor, J. S. *J. Med. Chem.* **2003,** *46,* 2973–2984.
(34) Martin, N. E.; et al. *Clin. Cancer Res.* **2004,** *10,* 5447–5454.
(35) Fu, H.; Moomaw, J. F.; Moomaw, C. R.; Casey, P. J. *J. Biol. Chem.* **1996,** *271,* 28541–28548.